Cell PRESS
Immunity
Article

Effector-like CD8$^+$ T Cells in the Memory Population Mediate Potent Protective Immunity

Janelle A. Olson,[1] Cameron McDonald-Hyman,[1] Stephen C. Jameson,[1,*] and Sara E. Hamilton[1,*]
[1]Department of Laboratory Medicine and Pathology, Center for Immunology, University of Minnesota Medical School, Minneapolis, MN, 55414, USA
*Correspondence: james024@umn.edu (S.C.J.), hamil062@umn.edu (S.E.H.)
http://dx.doi.org/10.1016/j.immuni.2013.05.009

SUMMARY

The CD8$^+$ memory T cell population is heterogeneous, and it is unclear which subset(s) optimally mediate the central goal of the immune system—protection against infection. Here we investigate the protective capacities of CD8$^+$ T cell subsets present at the memory stage of the immune response. We show that a population of CD8$^+$ T cells bearing markers associated with effector cells (KLRG1^{hi}, CD27^{lo}, T-bet^{hi}, Eomes^{lo}) persisted to the memory phase and provided optimal control of *Listeria monocytogenes* and vaccinia virus, despite weak recall proliferative responses. After antigen-specific boosting, this population formed the predominant secondary memory subset and maintained superior pathogen control. The effector-like memory subset displayed a distinct pattern of tissue distribution and localization within the spleen, and their enhanced capacity to eliminate Listeria involved specialized utilization of cytolysis. Together, these data suggest that long-lived effector CD8$^+$ T cells are optimal for protective immunity against certain pathogens.

INTRODUCTION

During a typical immune response, antigen-specific CD8$^+$ T cells undergo three characteristic phases: massive clonal expansion, contraction of effector cells, and establishment of memory. Considerable efforts have been made to define the factors that control generation of short-lived effector cells and establishment of long-lived memory (Jameson and Masopust, 2009; Kaech and Wherry, 2007; Masopust et al., 2007; Rutishauser and Kaech, 2010; Williams and Bevan, 2007). However, the memory pool that is formed as the result of an immune response is not homogeneous but rather contains distinct subsets of cells that differ in their functional, proliferative, trafficking, and survival characteristics (Jameson and Masopust, 2009; Seder et al., 2008). Some phenotypic features of memory cells define their trafficking characteristics (e.g., CCR7 and CD62L) or survival potential (e.g., the cytokine receptor chains CD127 and CD122), whereas others are used as correlative markers (such as the expression of KLRG1 on cells that are typically thought to be senescent) (Hikono et al., 2007; Joshi et al., 2007; Masopust et al., 2006a; Nolz et al., 2012; Sallusto et al., 1999; Sallusto et al., 2004; Sarkar et al., 2008). The best characterized division scheme for CD8$^+$ memory T cells is the paradigm of central and effector memory cells, based on CD62L and CCR7 expression. Central memory T (Tcm) cells, which express CD62L and CCR7, tend to localize to lymphoid tissues and are capable of robust recall proliferation and interleukin-2 (IL-2) production, whereas effector-memory T (Tem) cells, characterized by lack of CD62L and CCR7 expression, are prevalent at peripheral sites and can quickly become cytolytic, yet exhibit more limited recall proliferation function (Bachmann et al., 2005a; Bachmann et al., 2005b; Seder et al., 2008; Wherry et al., 2003; Wolint et al., 2004). Another division scheme for CD8$^+$ memory T cells was proposed by Hikono et al., who used expression of CXCR3, CD27, and a glycoform of CD43 as a basis for subset identification (Hikono et al., 2006). These markers subdivide the Tcm and Tem cell pools, offering refinement of functional properties within the memory-stage pool: for example, the CD27^{hi}CD43^{lo} subset becomes dominant over time and shows optimal recall proliferation—and hence was presumed to be functionally superior (Hikono et al., 2007).

These studies support the concept that the fully mature memory pool consists of long-lived CD8$^+$ T cells with a CD62L^{hi} CD27^{hi} CD43^{lo} KLRG1^{lo} CD127^{hi} phenotype, characterized by efficient recall proliferation. However, such findings do not necessarily mean that this population is optimal for immediate protective immunity—the intended goal of vaccination. Indeed, there is considerable controversy about which subset(s) of memory CD8$^+$ T cells are most potent for pathogen control. For example, in studies on CD8$^+$ T cell control of vaccinia virus, some groups proposed that Tcm cells are optimal for protection (Laouar et al., 2008; Wherry et al., 2003), whereas others proposed that Tem cells are the more potent subset (Bachmann et al., 2005a; Bachmann et al., 2005b). There is better consensus that Tcm cells, with their superior recall proliferative characteristics, are best suited for control of LCMV (Bachmann et al., 2005a; Bachmann et al., 2005b; Wherry et al., 2003) – but the mechanisms involved in control of this noncytopathic virus may not correspond to the responses needed to eliminate a pathogen that causes direct tissue damage.

Implicit in these studies is the idea that cells with effector-like properties—for example, cells with the KLRG1^{hi} CD62L^{lo} CD27^{lo} phenotype—play no role in protective immunity at the memory stage. Initially, this conclusion seems reasonable because effector cells are notable for their lack of recall

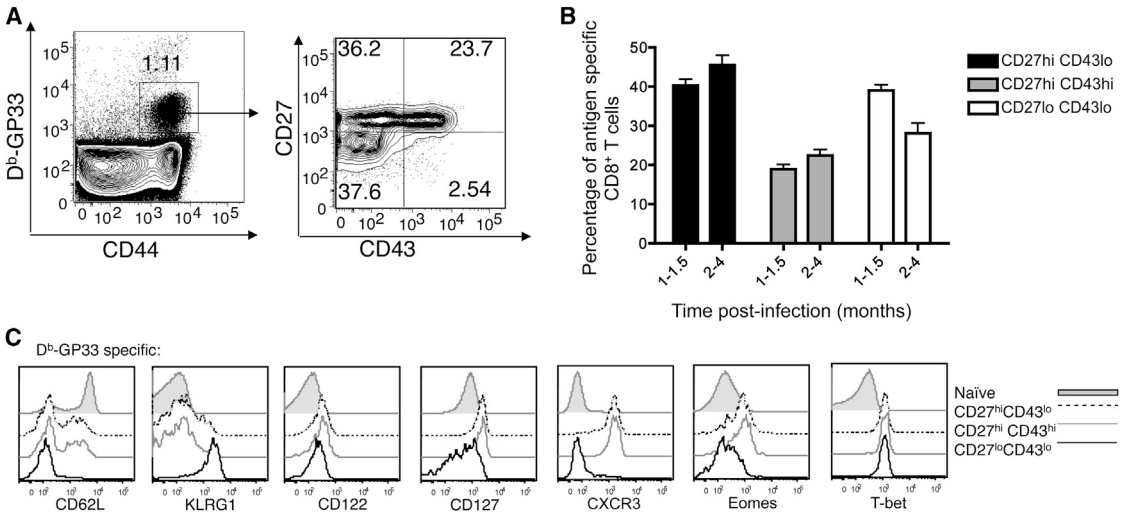

Figure 1. CD27^{lo} CD43^{lo} CD8^{+} Memory T Cells Display a Unique Phenotype

(A) Mice were infected with LCMV. One month after infection, splenocytes were stained for CD8^{+}, gp33-D^{b} tetramer, and the indicated markers. Data is representative of at least four experiments (n = 12).

(B) Compiled data from experiments in which mice were infected with LCMV, LM-OVA, or LM-B8R. At the indicated time periods, antigen-specific cells were identified (by using gp33-D^{b}, Ova-K^{b}, or B8R-K^{b} tetramers, respectively) and the frequency of indicated subsets was determined. Data is compiled from at least four experiments (n = 14 for 1–1.5 month period, n = 25 for 2–4 month period), presented as mean ± SEM.

(C) gp33-D^{b} tetramer-binding CD8^{+} T cells from spleen and lymph nodes were stained with the indicated markers 1 month after infection with LCMV. Data is representative of four experiments (n = 12). See also Figure S1.

proliferation and susceptibility to death, leading to loss of most effector-phenotype cells prior to the memory phase (Joshi et al., 2007; Kaech et al., 2003; Prlic and Bevan, 2008; Sarkar et al., 2008). Yet it is also notable that such studies find a small subset of cells with effector-like traits that persists for many months after a primary immune response. Furthermore, the size and durability of CD8^{+} T cells with effector-like properties is greatly enhanced following antigen-specific boosting of the CD8^{+} T cell pool (Jabbari and Harty, 2006; Masopust et al., 2006a; Sandau et al., 2010; Wirth et al., 2010b)—however, it remains controversial whether production of such cells by boosting enhances or diminishes the protective function of CD8^{+} T cells (Hansen et al., 2009, 2011; Huster et al., 2009; Jabbari and Harty, 2006; Nolz and Harty, 2011; Vezys et al., 2009; Wirth et al., 2010b).

In the current report, we examine the functional significance of cells with effector-like traits that persist to the memory phase. By cell sorting, we show that memory-stage cells, with a KLRG1^{hi}, CD127^{int}, CD27^{lo}, CD62L^{lo} phenotype, mediate rapid protective immunity against infection with vaccinia virus and *Listeria monocytogenes*, in spite of suboptimal recall proliferative capacity. This population is expanded and maintained long term following boosting, without losing their protective superiority. This "long-lived effector" subset shows distinct tissue localization (that can enhance encounter with pathogens) and uniquely takes advantage of cytolytic capacity in its control of Listeria. Together, these data suggest that immediate protective immunity against acute pathogen infection is best provided by cells with effector-like traits that persist to the memory phase, suggesting a different focus for vaccination strategies.

RESULTS

Three Subsets of Memory Cells Defined by CD27 and CD43 Expression Are Maintained Long Term after Systemic Infection

Studies testing whether protective immunity is best mediated by central or effector memory CD8^{+} T cells have led to contradictory findings (Bachmann et al., 2005a, 2005b; Jameson and Masopust, 2009; Laouar et al., 2008; Seder et al., 2008; Wherry et al., 2003). Hence we investigated an alternative subsetting system (based on expression of CD27 and an alternative glycoform of CD43), which was shown to accurately predict the memory CD8^{+} T cell recall response (Hikono et al., 2007). We first examined expression of these markers in antigen-specific CD8^{+} T cell populations persisting to the memory phase following a primary immune response against *Listeria monocytogenes* (LM) or LCMV. In keeping with previous studies (Hikono et al., 2007; Sandau et al., 2010), three main populations were observed: CD27^{hi} CD43^{lo}, CD27^{hi} CD43^{hi}, and CD27^{lo} CD43^{lo} subsets (Figure 1A). These three populations arose following systemic infection with LCMV or LM recombinants (Figure 1B; see also Figure S1A available online) and also developed after VV infection or LM delivered by the intranasal route (data not shown), suggesting the type and route of acute infection does not influence the formation of such subsets. Likewise, similar subsets were generated with priming of T cell receptor transgenic CD8^{+} T cells (Figure S1B) (Sandau et al., 2010), indicating that TCR affinity for antigen does not dictate differentiation into these different memory stage subsets. As reported previously (Hikono et al., 2007), the CD27^{hi} CD43^{lo} subset came to dominate the memory pool at later time points, but all three populations

were well represented for many months following a primary immune response (Figure 1B).

Examination of other cell surface markers revealed striking differences between these subsets. $CD27^{hi}$ populations (whether $CD43^{hi}$ or $CD43^{lo}$) contained $CD62L^{hi}$ and $CD62^{lo}$ subsets and displayed markers of typical memory $CD8^+$ T cells, including high expression of the cytokine receptor chains CD122 and CD127, with low expression of the "effector cell" marker, KLRG1 (Figure 1C). Hence, prototypical Tcm and Tem cell populations are both contained in the $CD27^{hi}$ subset. In contrast, the $CD27^{lo}$ $CD43^{lo}$ pool showed a substantially different phenotype, being $CD127^{int}$ and $KLRG1^{hi}$. Furthermore, $CD27^{lo}$ $CD43^{lo}$ cells exhibited high expression of the transcription factor T-bet but minimal expression of the related factor Eomes, features which are also associated with effector cells (Banerjee et al., 2010; Intlekofer et al., 2005; Joshi et al., 2007). At first glance, this phenotype suggests similarity between the $CD27^{lo}$ $CD43^{lo}$ subset and short-lived effector cells (SLEC) (Joshi et al., 2007). However, in contrast to the drastic downregulation of CD127 reported for short-lived effector cells (Joshi et al., 2007; Kaech et al., 2003; Obar and Lefrançois, 2010), the memory stage $CD27^{lo}$ $CD43^{lo}$ population expressed CD127 at levels similar to naive $CD8^+$ T cells (albeit at lower levels than either $CD27^{hi}$ population) (Figure 1C; Figures S1C and S1D). Hence this population is more similar to the KLRG-1, CD127 double-positive population reported by others (Obar and Lefrançois, 2010).

The $CD27^{lo}$ $CD43^{lo}$ Subset Shows Optimal Protection against Listeria and Vaccinia Infection

Previous data suggest that the $CD27^{lo}$ $CD43^{lo}$ pool was poor at recall proliferation (Hikono et al., 2007), and several phenotypic features of this pool (high expression of KLRG1, low expression of CD27, and CD127) have been correlated with senescent $CD8^+$ T cells (Baars et al., 2005; Heffner and Fearon, 2007; Hikono et al., 2007). Furthermore, this population (in contrast to the $CD27^{hi}$ memory subsets) lacked expression of CXCR3 (Figure 1C), which might be expected to limit their ability to promptly traffic to sites of inflammation. Hence, one might anticipate that $CD27^{lo}$ $CD43^{lo}$ cells would show inferior protection compared to the prototypical Tem and Tcm cell populations present in the $CD27^{hi}$ pool. Yet this has not been directly tested. Thus, we explored how CD27, CD43 defined subsets performed in protection assays by using a heterologous protection model (Figure 2A). Mice were primed with LCMV, memory populations were sorted, and equivalent numbers of gp33-D^b-specific $CD8^+$ T cells from each memory subset adoptively transferred into normal recipients. Host animals were infected with LM-gp33, and 5 days later the donor cell expansion and LM clearance were determined.

Surprisingly, the $CD27^{lo}$ $CD43^{lo}$ subset provided significantly greater protective immunity than either of the $CD27^{hi}$ memory $CD8^+$ T cell populations (Figure 2B). Interestingly, the enhanced protection provided by the $CD27^{lo}$ $CD43^{lo}$ subset did not correspond to the magnitude of the donor cell response during challenge—indeed, fewer donor cells were isolated from animals receiving the $CD27^{lo}$ $CD43^{lo}$ pool (Figure 2C). This likely results from less efficient adoptive transfer "take" of $CD27^{lo}$ $CD43^{lo}$ cells initially (Figure S2A), together with reduced expansion of this subsets after antigen encounter (in keeping with previous studies [Hikono et al., 2007]). Regardless of mechanism, our findings indicate that the size of the donor cell response did not accurately predict LM elimination.

Similar results were observed when OT-I memory T cell subsets were tested for protection against LM-OVA (Figure S2B), ruling out potential differences in TCR affinity within the memory subsets as a basis for distinct protective capacity. Also, studies using titrated donor cell transfers indicated that low numbers of the $CD27^{lo}$ $CD43^{lo}$ subset were more effective at protection than an excess of $CD27^{hi}$ $CD43^{lo}$ or $CD27^{hi}$ $CD43^{hi}$ cells (Figure S2C).

Kinetic studies (using a homologous LM-OVA protection assay) indicated that the $CD27^{lo}$ subset continued to reduce the pathogen burden at day 7, outperforming both CD27 subsets (Figure 2D). Whereas the $CD27^{hi}CD43^{lo}$ population also offered substantial immunity by day 7, $CD27^{hi}CD43^{hi}$ cells were much more variable in mediating LM clearance. None of the transferred subsets were protective by the day 3 time point, indicating that subsequent differences in donor-cell expansion did not relate to differential early bacterial clearance. Together, these data suggest that the $CD27^{lo}$ $CD43^{lo}$ subset offers the most potent and efficient protective immunity. In contrast, the $CD27^{hi}$ subsets (regardless of CD43 expression), offered considerably weaker protective immunity, despite the fact that these subsets include prototypical Tcm and Tem cell populations.

It was possible that optimal protection by the $CD27^{lo}$ $CD43^{lo}$ memory pool was unique to assays involving LM control. Therefore, we also investigated protective immunity against vaccinia virus (VV), after priming with LM-B8R (a recombinant LM strain bearing an immunodominant VV epitope). Furthermore, we analyzed viral control in a nonlymphoid organ (the ovary, which forms a site for intense VV replication (Karupiah et al., 1990)) rather than the spleen and liver analyzed for LM control. Again, the $CD27^{lo}$ $CD43^{lo}$ population offered superior pathogen elimination, compared to the other memory subsets (Figure 2E). Therefore, in diverse models of acute pathogen infection, $CD27^{lo}$ $CD43^{lo}$ $KLRG\text{-}1^{hi}$ phenotype cells provide optimal protection, compared to the classic memory phenotype $CD8^+$ T cell pools.

Boosting Increases the Frequency of Protective $CD27^{lo}$ $CD43^{lo}KLRG1^{hi}$ $CD8^+$ Cells

Although the $CD27^{lo}$ $CD43^{lo}$ subset persists for many months following priming (Figure 1), these cells eventually decline (Hikono et al., 2007). Comparison between P14 memory $CD8^+$ T cells at 1 month versus ~1 year after priming demonstrated almost complete loss of this subset in the "old" memory pool (Figure S3A). Preliminary studies indicated that challenge of these immunized mice resulted in efficient LM-gp33 control, regardless of the time after priming (data not shown)—however, because such animals have a large population of memory P14 $CD8^+$ T cells (>5% of the $CD8^+$ T cell pool), we further assayed the protective function of "old" versus "young" P14 memory cells by using adoptive transfer assays. Interestingly, aged memory P14 $CD8^+$ T cells showed considerably weaker per-cell protection against LM-gp33 (Figure S3B). Although there may be diverse reasons for this outcome, such results are consistent with the $CD27^{lo}$ $CD43^{lo}$ subset offering superior control against Listeria.

These findings raise the question of whether the size and persistence of the $CD27^{lo}$ $CD43^{lo}$ subset can be extended. Interestingly, previous work showed that antigen-specific boosting

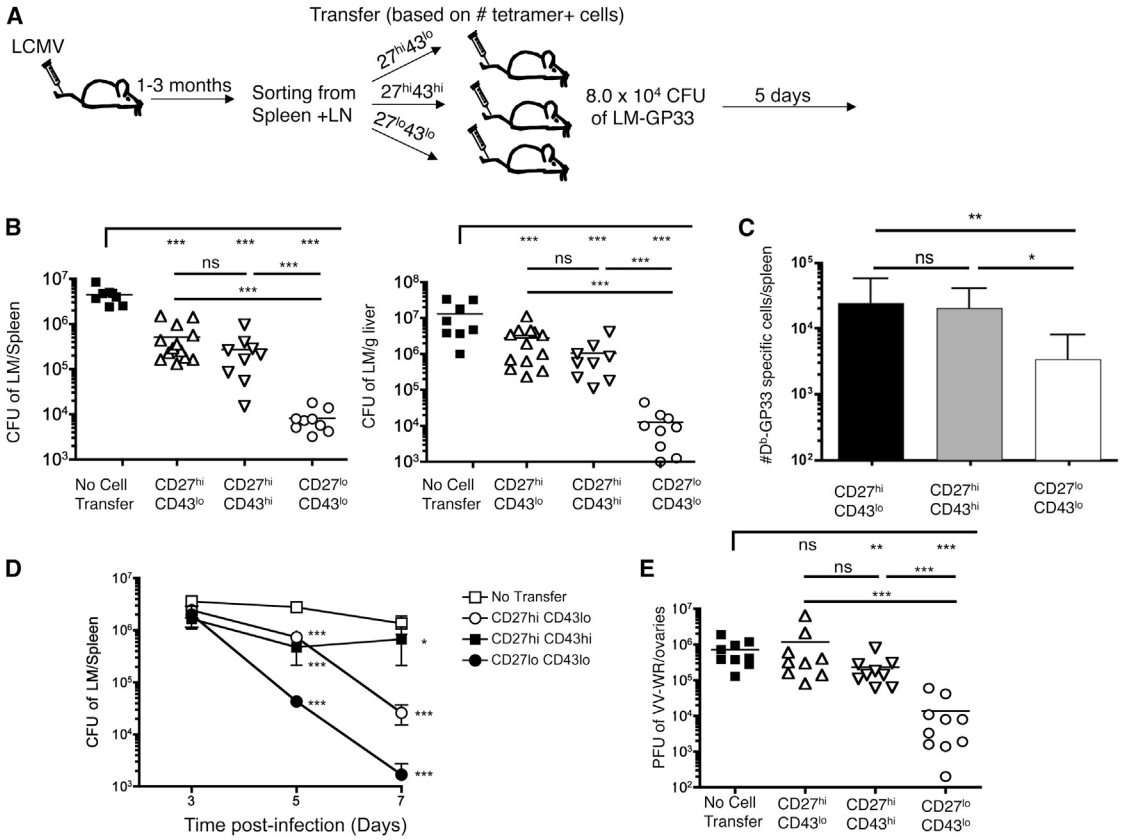

Figure 2. Robust Protection by CD27^{lo} CD43^{lo} Memory Cells

(A) Experimental schematic. CD8$^+$ CD44^{hi} LCMV memory cells were sort purified 1–3 months after infection according to CD27 and CD43 expression, and each population was injected into naive recipients, such that an equal number of gp33-D^b tetramer-binding cells were adoptively transferred.

(B and C) Mice were challenged with LM-gp33. Five days after challenge, the number of CFU of LM in the spleen and liver was determined (B) and the number of gp33-D^b specific CD8$^+$ T cells in the spleen quantified (C). Data are compiled from three independent experiments. Data in (B) shows individual CFU, with mean values indicated by a line, while the data in (C) shows mean ± SD. p values are represented as follows: ***p < 0.001; **p < 0.01; *p < 0.05.

(D) Mice were primed with *ActA* LM-OVA, and at least 1 month later memory subsets were sorted and 3 × 10^4 cells of each subset adoptively transferred per recipient. Host animals (and "No-transfer" controls) were infected with virulent LM-OVA and protection determined at 3, 5, or 7 days after infection. Data are compiled from three experiments and shown as mean ± SEM. Statistical analysis is represented by asterisks, indicating significant changes in comparison with the no-transfer group for each time point.

(E) A similar experimental plan to (A) was used, except that mice were infected with LM-B8R to induce a B8R-K^b specific response and, following transfer of sorted memory CD8$^+$ T cells, recipient mice were challenged with VV-WR. Three days after VV-WR infection, the number of PFU of VV in the ovaries was determined. Individual mice compiled from three experiments are shown. See also Figure S2.

increases the number and duration of CD27^{lo} KLRG1$^+$ cells within the antigen-specific CD8$^+$ memory T cell pool (Masopust et al., 2006a; Sandau et al., 2010; Wirth et al., 2010a, 2010b). However, it was not clear whether these cells would show efficient protective functions, because some studies suggest that boosting decreases the fitness of CD8$^+$ T cells and impairs their ability to respond toward certain pathogens (Nolz and Harty, 2011; Wirth et al., 2010b).

To investigate this issue, we used an efficient prime-boost strategy involving immunization with OVA peptide-coated cells, followed by boosting with LM-OVA (Badovinac et al., 2005; Pham et al., 2010). In such approaches, very few effector cells are produced in the primary (1°) response, with the vast majority of antigen-specific cells rapidly adopting a central memory phenotype (Badovinac et al., 2005; Pham et al., 2010) (data not shown), and these memory cells quickly become competent to undergo an efficient secondary (2°) response (Badovinac et al., 2005; Pham et al., 2010). We selected this rapid prime-boost system because it has been shown to induce potent 2°CD8$^+$ T cell memory, capable of protecting against viral, bacterial, and parasitic infections (Pham et al., 2010). At least 3 months after the last immunization, OVA-K^b-specific cells were analyzed. Secondary memory cells showed a greatly expanded population of CD27^{lo} CD43^{lo} cells, with few CD27^{hi} CD43^{lo} cells (and virtually no CD27^{hi} CD43^{hi} cells) (Figures 3A and 3B), in contrast to the diverse populations present in the 1° memory CD8$^+$ pool (which were analyzed in parallel, following immunization with LM-OVA alone). The 2°CD27^{lo} CD43^{lo} pool was even more markedly reduced for expression of Eomes, but was similar to its counterpart in the 1° memory pool in being KLRG1^{hi} T-bet^{hi}, CD62^{lo} and CXCR3^{lo}, and CD127^{int} (Figure 3C). Therefore, boosting greatly enriches the frequency of the CD27^{lo} CD43^{lo}

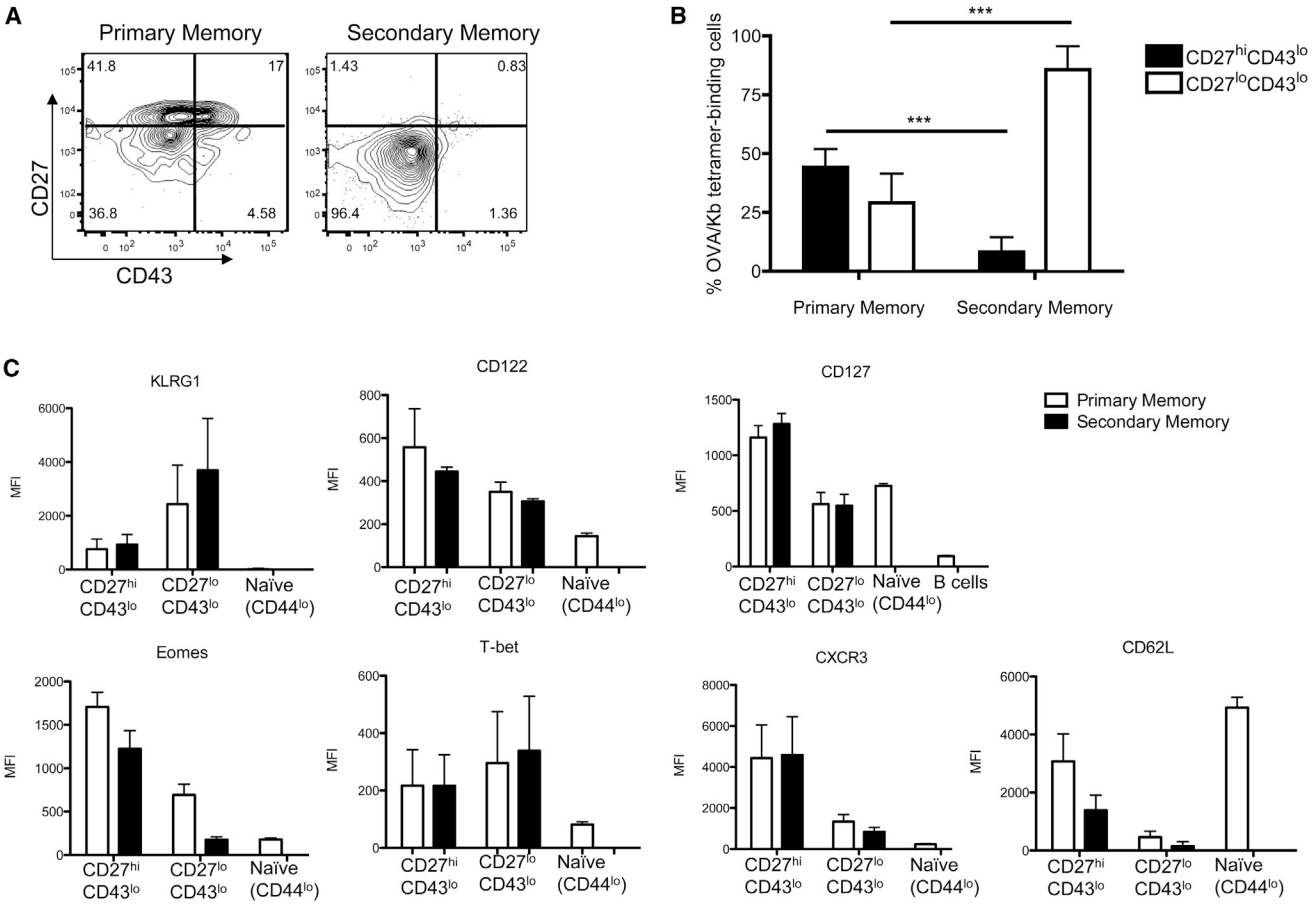

Figure 3. CD27^{lo} CD43^{lo} Cells Are Strongly Increased with Boosting

(A) Example staining of the frequency of K^{b}-OVA+ cells expressing CD27 and CD43, 3–4 months after infection with ActA LM-OVA (primary memory) or 3–4 months after boosting with LM-OVA (secondary memory). Data is representative of three experiments (n = 9).

(B) Compiled data of the frequency of CD27^{hi} CD43^{lo} and CD27^{lo} CD43^{lo} within K^{b}-OVA+ cells. Error bars show the average ± SD from three experiments (n = 9).

(C) MFI of phenotypic markers on primary and secondary memory populations. Naive (CD44^{lo}) CD8^{+} T cells and/or B cells (CD19^{+}) are also included for comparison. Error bars show the mean ± SD from three experiments (n = 9). See also Figure S3.

population surviving to the 2° memory stage, without changing their major phenotypic features.

Next, we assessed the protective capacity of 2° memory subsets, in comparison with cells from the 1° memory pool. The lack of CD27^{hi} CD43^{hi} cells precluded assessment of this subset in the 2° memory pool, and our studies on the 1° memory population suggested similar protection by CD27^{hi} CD43^{hi} and CD27^{hi} CD43^{lo} populations (Figure 2). Hence, we sorted CD27^{hi} CD43^{lo} and CD27^{lo} CD43^{lo} subsets from 1° or 2° memory pools and adoptively transferred these cells into normal recipients, which were then challenged with virulent LM-OVA.

As expected, the 1° memory CD27^{lo} CD43^{lo} population displayed superior protective capacity compared to prototypical memory cells (CD27^{hi} CD43^{lo}), and similar outcomes were observed for the 2° memory subsets (Figure 4A). Once again, efficient protection by the secondary memory CD27^{lo} CD43^{lo} subset did not correlate with enhanced expansion of this population (Figure 4B). Hence, these data suggest boosting expands the number of CD27^{lo} CD43^{lo} memory CD8^{+} T cells without eroding their protective capacity.

The CD27^{lo} Memory CD8^{+} T Cell Subset Shows Differential Tissue Localization and Compartmentalization

Previous studies have shown that blood-borne LM initially infects macrophages in the splenic red pulp and marginal zone (Aoshi et al., 2009) and that initial memory CD8^{+} T cell encounter with LM-infected cells might take place in the red pulp (Bajénoff et al., 2010). Furthermore, short-lived effector cells selectively occupy the red pulp (Jung et al., 2010). Hence, we considered whether CD27^{lo} CD43^{lo} KLRG-1^{hi} memory cells showed preferential localization within the spleen. To analyze this, we intravenously injected mice with fluorescent anti-CD8^{+} antibody and isolated tissues after a brief delay: This technique labels CD8^{+} T cells exposed to the blood (including the splenic red pulp) but does not label cells in tissue parenchyma (including the white pulp) (Anderson et al., 2012; Galkina et al., 2005; Teijaro et al., 2011). Interestingly, the CD27^{lo} CD43^{lo} pool was selectively enriched in the red pulp, whereas the CD27^{hi} CD43^{lo} population showed preferential localization to the white pulp (Figures 5A and 5B). This asymmetry in red and white pulp distribution

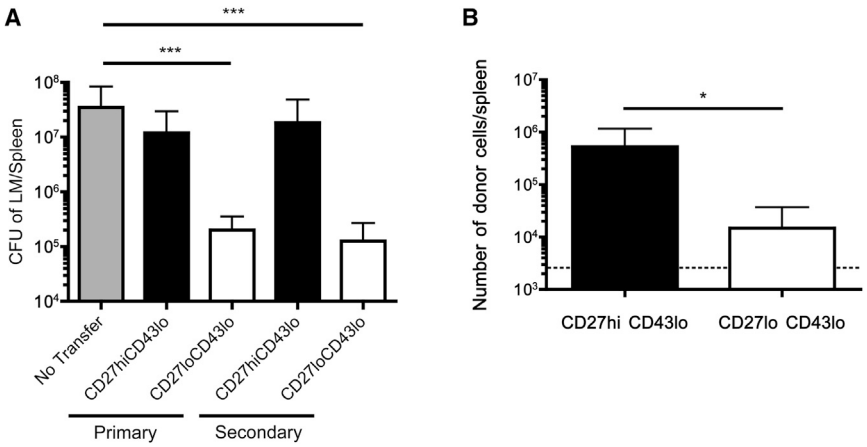

Figure 4. Boosting Increases the Number of Protective Memory Cells

$CD27^{hi}$ $CD43^{lo}$ and $CD27^{lo}$ $CD43^{lo}$ phenotype memory $CD8^+$ T cells were sorted from primary and secondary memory mice 2.5–3.5 months after the last antigen stimulation. Equal numbers of OVA-K^b tetramer staining cells were transferred into normal recipients, which were challenged with LM-OVA 1 day later. Five days following LM-OVA challenge, animals were sacrificed and (A) CFU of LM was determined in the spleen.

(B) The expansion of donor $CD27^{hi}$ $CD43^{lo}$ and $CD27^{lo}$ $CD43^{lo}$ secondary memory cells was determined in the spleen 5 days after LM-OVA challenge. The dotted line indicates the limit of detection. Data are shown as mean ± SD and are compiled from two independent experiments.

was also observed for memory subsets after adoptive transfer (Figure S4), and hence might contribute to the differences in protective immunity documented above. We also examined the frequency of the $CD27^{lo}$ $CD43^{lo}$ population in other tissues. Although this subset was 30%–40% of the splenic memory pool (Figure 1B), it constituted around 75% of circulating memory cells, yet was largely excluded from lymph nodes (as expected from the lack of CD62L expression) (Figure 5C). $CD27^{lo}$ memory cells constituted the vast majority of antigen-specific cells in the small intestine IEL and LP compartments (Figure 5C), as expected from earlier work (Masopust et al., 2006b). These cells express CD43 (Masopust et al., 2006b) (data not shown) and the extent of their similarity to $CD27^{lo}$ cells in lymphoid tissues is not clear, but these findings support the conclusion that localization of the $CD27^{lo}$ memory $CD8^+$ T cell pool is optimal for prompt engagement with invading pathogens.

Superior Protection against LM Depends on Cytolytic Potential of the $CD27^{lo}$ $CD43^{lo}$ Subset

Recall expansion is frequently used as a parameter of memory $CD8^+$ T cell function and is often assumed to correspond to potency in protective immunity. However, our data shows that recall proliferation of primary and secondary memory $CD8^+$ T cell subsets did not predict pathogen control (Figures 2 and 4). What then accounts for the enhanced protection mediated by the $CD27^{lo}$ $CD43^{lo}$ pool? To address this, we first assessed the ability of primary memory subsets to produce inflammatory cytokines. Antigen induced production of interferon-γ (IFN-γ) (Figure S5A) and tumor necrosis factor (TNF) (data not shown) was similar for all three CD27, CD43 defined subsets, assessed after cell sorting and in vitro activation with specific peptide-MHC. This finding contrasts with a recent study suggesting that $CD27^{lo}$ memory $CD8^+$ T cells exhibit impaired induction of IFN-γ compared to $CD27^{hi}$ cells (Nolz et al., 2012) but supports conclusions from earlier studies (Hikono et al., 2007; Sandau et al., 2010). Memory $CD8^+$ T cells can release IFN-γ in response to IL-12 and IL-18, and this may contribute to pathogen clearance in a non-antigen-specific manner (Berg et al., 2003; Kambayashi et al., 2003). However, that function was also similar for all three subsets defined by using CD27 and CD43 (Figure S5B). We also considered that the $CD27^{lo}$ $CD43^{lo}$ $KLRG1^{hi}$ subset may exhibit greater functional avidity (i.e., sensitivity to low dose peptide-MHC ligand) (Slifka and Whitton, 2001). However, when tested for upregulation of CD69, IFN-γ, and CD107a (a marker of degranulation), we observed similar dose responses for $KLRG1^{hi}$ and $KLRG1^{lo}$ memory subsets (Figure S5C).

Cytolytic ability is important for function of $CD8^+$ T cells during many infections—for example, $Prf1^{-/-}$ memory $CD8^+$ T cells (lacking Perforin expression) are approximately five times less active on a per cell basis in the clearance of LM (Messingham et al., 2003). Previous studies reported that $CD27^{lo}$ $CD43^{lo}$ cells (but not other memory subsets) express Granzyme B at steady state (Hikono et al., 2007; Sandau et al., 2010), and we confirm this finding (Figures 6A and 6B). However, the functional significance of cytolysis has not been assessed in these memory subsets. To evaluate this, we infected wild-type (WT) or $Prf1^{-/-}$ mice with attenuated LM-OVA and, after memory differentiation, sorted CD27, CD43 subsets (which developed similarly in both types of mice; data not shown). Each subset was transferred at equal number into WT mice followed by homologous challenge with virulent LM-OVA, and protection was monitored 5 days after infection. As expected, the $CD27^{lo}$ $CD43^{lo}$ memory subset isolated from normal mice offered significantly better protection than the other memory subsets (Figure 6C, left). However, this protective advantage was completely lost when the $CD27^{lo}$ $CD43^{lo}$ subset from $Prf1^{-/-}$ animals was analyzed. Surprisingly, this requirement for cytolytic potential was uniquely invested in the $CD27^{lo}$ $CD43^{lo}$ population—Perforin deficiency did not compromise the ability of either $CD27^{hi}$ subset to mediate partial protection against LM infection (Figure 6C). This finding suggests that cytolysis is critical for the ability of $CD27^{lo}$ $CD43^{lo}$ cells to mediate rapid protection against LM, but also reveals that this effector function is uniquely invested in the $CD27^{lo}$ $CD43^{lo}$ pool, with the protective function of other memory subsets being Perforin independent. Such findings suggest specialized distribution of key effector functions to certain memory $CD8^+$ T cell subsets.

DISCUSSION

The goal of successful vaccination is rapid control of infection–the timing of which could make the difference between

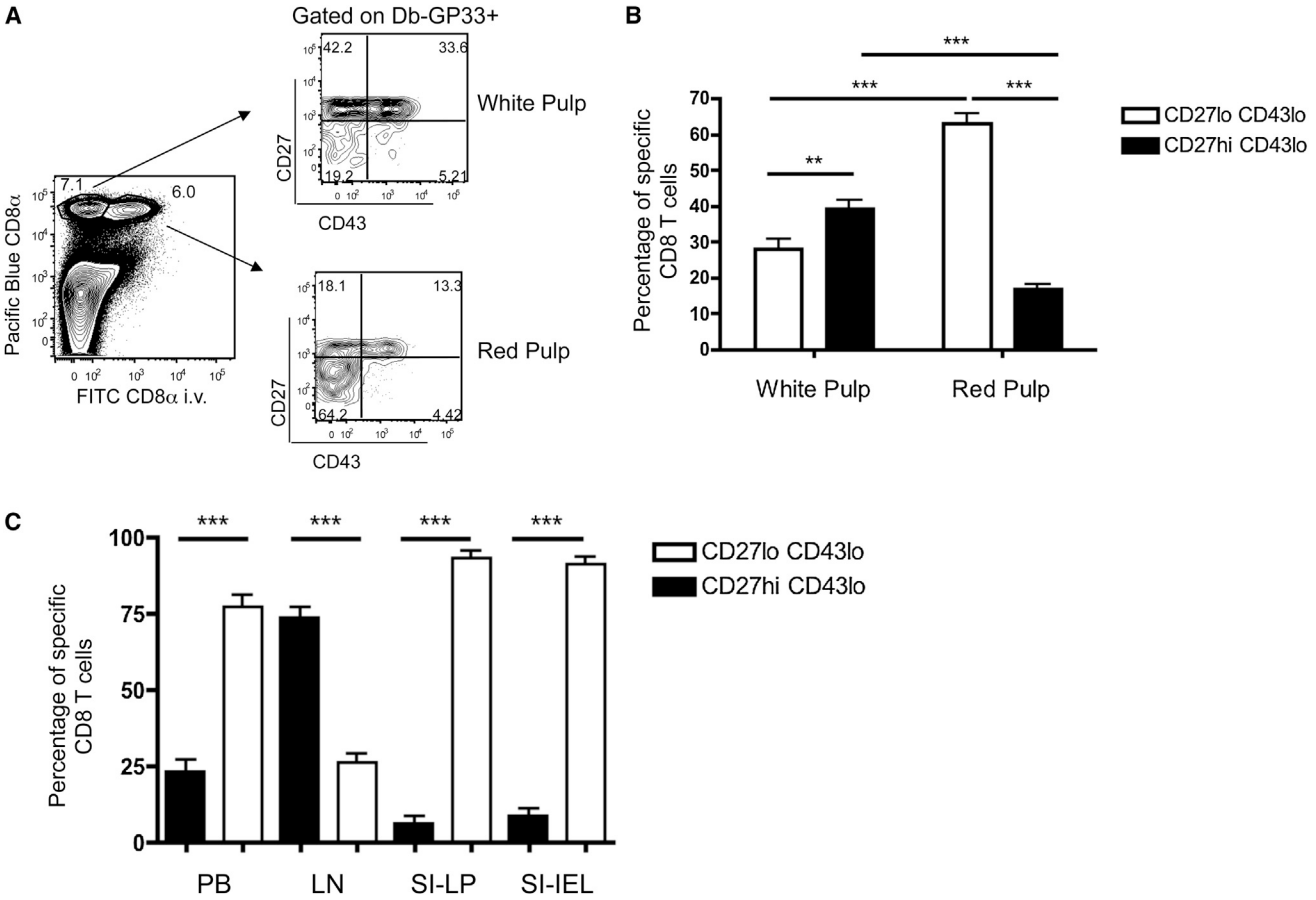

Figure 5. CD27^{lo} CD43^{lo} Memory Cells Localize to the Red Pulp and Nonlymphoid Sites

(A) Discrimination of splenic red and white pulp by injection of anti-CD8$^{+}\alpha$ antibody. CD27 and CD43 expression on gp33-D^{b} tetramer-binding CD8^{+} T cells within each compartment is shown, from mice infected 1–2 months earlier with LCMV. A representative example is displayed.

(B) Compiled data showing the localization of CD27^{hi} CD43^{lo} and CD27^{lo} CD43^{lo} memory CD8^{+} T cells, 1–2 months after LM-OVA or LCMV infection (gating on OVA-K^{b} and gp33-D^{b} tetramer-binding cells, respectively) (n = 13). The data represent mean ± SEM.

(C) The frequency of CD27^{hi} or CD27^{lo} antigen-specific memory CD8^{+} T cells in the blood, LN, IEL, and LPL compartments was determined, 1–2 months after LCMV or LM-OVA infection. Error bars show compiled data from four experiments (n = 9) and are shown as mean ± SEM. See also Figure S4.

asymptomatic clearance or severe tissue damage and death. Yet despite decades of work on memory T cell responses to pathogens, surprisingly little is known about which memory CD8^{+} T subsets mediate optimal protective immunity. In this report, we focus on a memory CD8^{+} T cell subset that develops during varied immune responses. The phenotypic traits of this Tem subset (CD62L^{lo}, CD27^{lo}, KLRG-1^{hi}, T-bet^{hi}, Eomes^{lo} and low CD127 expression) resemble those of short lived effector cells, and this feature (together with the reduced long-term survival and weaker recall proliferation of this subset), has lead to the conclusion that such cells may be senescent (Baars et al., 2005; Heffner and Fearon, 2007; Hikono et al., 2007; Nolz et al., 2012). Yet we found that this CD27^{lo} CD43^{lo} memory subset provides the most robust resistance against certain acute bacterial (Listeria) and viral (vaccinia) infections and demonstrated that this protective population is expanded and maintained in the secondary memory pool (following rapid prime-boost immunization).

Many studies use recall proliferation as an index for a "useful" memory T cell population, with the tacit assumption that rapid production of numerous effector cells is a key element in control of a rapidly replicating pathogen. However, our finding that the CD27^{lo} CD43^{lo} memory CD8^{+} T cell pool excels at protection despite displaying modest recall proliferation brings this correlation into question. Rather than superior expansion, cytolytic potential of the CD27^{lo} CD43^{lo} pool was critical for their enhanced control of LM while, surprisingly, this function played little part in the more moderate protection mediated by CD27^{hi} memory subsets. Studies from Harty's group showed that bulk Perforin-deficient memory CD8^{+} T cells displayed a reduced per-cell capacity to control LM (Messingham et al., 2003): Our data suggest that reliance on killing does not apply equally to all memory cell subsets but rather reflects a selective utilization of cytolysis by the highly protective CD27^{lo} CD43^{lo} population. Furthermore, the CD27^{lo} CD43^{lo} memory pool showed preferential localization to the red pulp of the spleen, which forms a major site for encounter with blood-borne pathogens, including Listeria (Aoshi et al., 2009) and is implicated as a key site for the initial encounter of memory CD8^{+} T cells with LM-infected macrophages (Bajénoff et al., 2010). Previous studies found preferentially localization

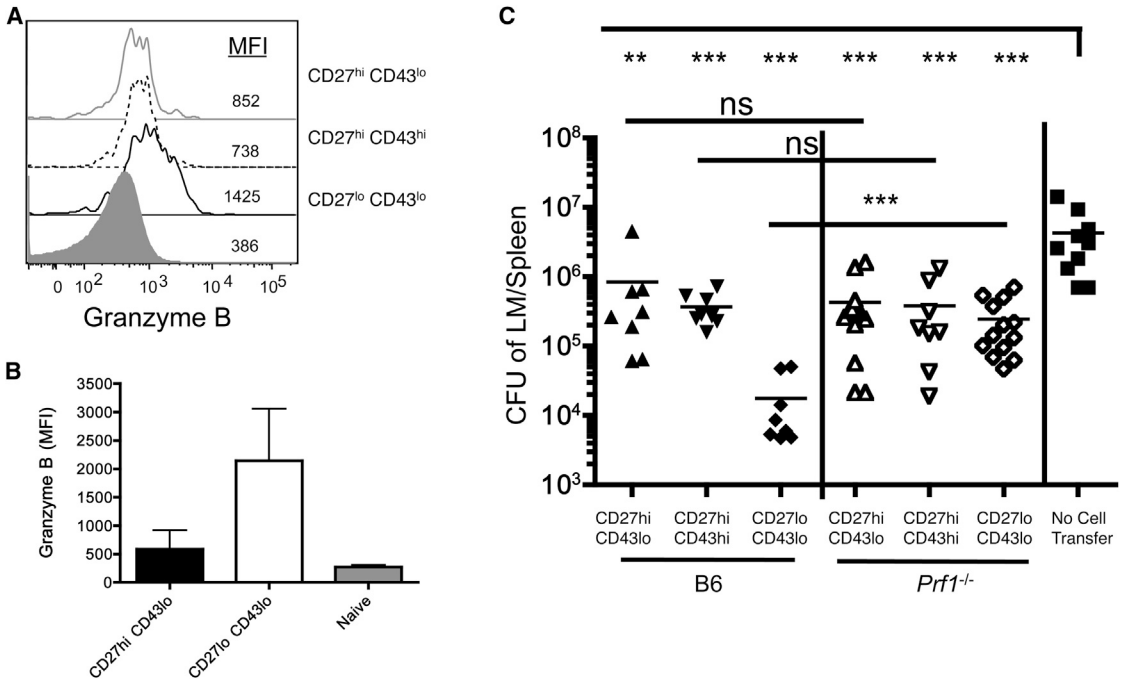

Figure 6. Cytolytic Function Is Required for Enhanced Protective Immunity by CD27^{lo} CD43^{lo} Cells

(A) Intracellular staining of granzyme B by indicated memory subsets of gp33-D^{b} tetramer-binding cells, 30 days after LCMV infection.

(B) Granzyme B expression in OVA-K^{b} tetramer-staining memory CD8^{+} T cell subsets isolated from animals immunized 3–4 months earlier with *ActA* LM-OVA. Naive (CD44^{lo}) CD8^{+} T cells are included as a control. Data are shown as mean ± SD (n = 9).

(C) Memory subsets were sorted from *ActA* LM-OVA infected B6 or Perforin-deficient (*Prf1*$^{-/-}$) mice, 1–2 months after infection. Cells were transferred in equal number into B6.SJL recipients, which were then challenged with LM-OVA. Five days after infection, the number of CFU in the spleen was calculated. Symbols represent individual mice compiled from three different experiments. See also Figure S5.

of effector cells and (at later time points) effector-memory cells to the red pulp (Jung et al., 2010): Our data extend those observations, demonstrating that the highly protective CD27^{lo} CD43^{lo} memory CD8^{+} T cell subset is optimally placed to encounter microbes in the blood. Such findings fit with the concept of poly-functionality—in which optimally protective memory T cells display multiple specialized traits (Seder et al., 2008)—but do not exclude a model in which distinct pools of memory T cells cooperate for protection. For example, in our studies rapid pathogen control was mediated by CD27^{lo} CD43^{lo} cells, yet the poor expansion of this subset suggests that progeny of the CD27^{hi} population will dominate in the recall effector pool—the protective capacity of the CD27^{hi} pool, although delayed, may be essential for elimination of residual infection.

Our data tested protection against LM and VV—does the CD27^{lo} CD43^{lo} long-lived effector pool mediate protection against other pathogens? By using similar rapid prime-boost approaches, Harty and colleagues showed that resistance to Listeria, vaccinia, influenza, and malaria were all enhanced (Badovinac et al., 2005; Pham et al., 2010): Those studies did not define the full phenotype of the secondary memory population, nor test protection by distinct memory subsets, but the predominance of CD27^{lo}, CD43^{lo}, KLRG-1^{hi}, CD127^{int} cells that we detect in prime-boosted animals (Figure 3) suggests that these cells are a likely source for protection in those studies. Alternatively, it is likely that responses to some infectious agents will involve distinct protection mechanisms, mediated by different memory subsets. For example, several studies indicate central memory CD8^{+} T cells are best suited for control of LCMV (Bachmann et al., 2005a, 2005b; Nolz and Harty, 2011; Wherry et al., 2003), and the superlative recall expansion of Tcm cell pool may be critical for keeping pace with rapidly spreading virus. In our hands, the CD62L^{hi} central-memory phenotype population was exclusively found in the CD27^{hi} memory CD8^{+} T cell subset, and hence this pool may be key for responses that require efficient lymph node entry (Nolz and Harty, 2011). Preliminary data indicate that all three CD27, CD43 defined memory subsets offer similar, modest control of LCMV clone 13 infection (data not shown), but further studies will be required to fully assess their protective capacity compared to ''classic'' central memory CD8^{+} T cells. Hence, our data should not be taken to mean that CD27^{lo} CD43^{lo} are superior for control of all pathogen infections. Prior studies testing protection by bulk secondary memory CD8^{+} T cells showed improved protection against LM and vaccinia virus (in keeping with our findings on the elevated frequency of the CD27^{lo} CD43^{lo} subset), but reduced control of MHV and LCMV Clone 13 (Nolz and Harty, 2011). Hence, control of different microbes may rely on the diversity of subsets within the memory pool (especially following a primary immune response). It will also be important to determine whether distinct memory CD8^{+} T cell populations are optimal at control of systemic versus local (e.g., mucosal) infections.

Nevertheless, our studies suggest production and preservation of CD27^{lo} CD43^{lo} cells will be useful as a vaccine goal for

various pathogens. Based primarily on studies of short-lived effector cells, it has been proposed that CD27^{lo}, KLRG1^{hi} phenotype cells are a transient, senescent pool (Baars et al., 2005; Heffner and Fearon, 2007; Hikono et al., 2007; Nolz et al., 2012), although some studies reported that memory populations enriched in cells of this phenotype survive and undergo recall responses similarly to the CD27^{hi} KLRG1^{lo} pool (Prlic et al., 2012). It is important to stress that, in contrast to short-lived effectors, the CD27^{lo} CD43^{lo} KLRG1^{hi} memory pool studied here expresses CD127 (although at reduced levels compared to CD27^{hi} subsets) and CD122, cytokine receptor chains critical for response to IL-7 and IL-15 respectively, and that this population persists > 4 months after primary and secondary infections (Figures 1 and 3). However, we did confirm that the CD27^{lo} CD43^{lo} population declines considerably by 1 year after priming and that this accompanies a loss in per-cell protective capacity by the ''aged'' memory pool (Figure S3). Interestingly, recent studies suggest that cells with an overlapping phenotype (CD27^{lo} CD62^{lo}) constitute a death-intermediate pool of memory cells, being an apoptosis-prone, nonfunctional population derived from homeostasis of the central memory CD27^{hi} subset (Nolz et al., 2012). Also, some studies suggest ''unhelped'' memory CD8$^+$ T cells (those primed in the absence of CD4 help) display a related phenotype, and have impaired functional traits (Edwards et al., 2013; Intlekofer et al., 2007). In contrast, our studies indicate that the CD27^{lo} population exhibits cytokine production similar to CD27^{hi} cells, undergoes recall proliferation (albeit less efficiently than other memory subsets), and mediates excellent protective function. Furthermore, the high frequency of CD27^{lo} CD43^{lo} CD8$^+$ T cells in the secondary memory pool makes it unlikely that they are derived from rare central memory cells in boosted animals. It will be important to determine whether immunization strategies such as the rapid prime boost approach employed here, affects the nature of CD27^{lo} CD43^{lo} memory CD8+ T cell homeostasis.

In summary, our studies indicate that cells with effector-like traits persist to the memory phase and constitute the most protective pool for control of certain infections. This subset shows unique tissue localization and utilization of cytolysis in pathogen control, and the fact that this subset is substantially expanded by boosting suggests such cells should be a desired focus of vaccination approaches.

EXPERIMENTAL PROCEDURES

Mice

We purchased 6- to 12-week-old female C57BL/6 and B6.SJL mice from the National Cancer Institute. TCR transgenic mice (P14 (Pircher et al., 1991)—a kind gift of Dr. David Masopust, University of Minnesota, and OT-I (Hogquist et al., 1994)—were maintained on a B6.PL (Thy-1.1) background. Perforin-deficient mice were obtained from Jackson Laboratories and provided by Dr. Stephen McSorely, University of California Davis. All mice were maintained in SPF conditions, and all mouse protocols were approved by the University of Minnesota Institutional Animal Care and Use Committee.

Bacterial and Viral Infections

Recombinant LM strains LM-OVA (virulent and *ActA* attenuated) and LM-gp33 were provided by Hao Shen (University of Pennsylvania School of Medicine, Philadelphia, PA) and John Harty (University of Iowa) and have been described (Pope et al., 2001). In addition, a novel strain of virulent LM-gp33 was kindly provided by Dr. Dietmar Zehn (University of Lausanne, Switzerland). Attenuated strain LM-B8R (expressing the B8R CD8$^+$ epitope from vaccinia virus) (Hamilton et al., 2010) was provided by Dr. Ross Kedl (National Jewish Medical Research Center, University of Colorado, Denver, CO). LCMV (Armstrong) was provided by Dr. David Masopust (University of Minnesota).

LM was grown in tryptic soy broth with 50 μg/ml streptomycin to an OD_{600} of ~0.1. For LM-OVA challenges, 8 × 10^4 CFU were injected intravenously (i.v.). For primary infection with attenuated LM-OVA or LM-B8R, 3–6 × 10^6 CFU were injected i.v. Primary infection with LCMV Armstrong was with 2 × 10^5 PFU injected intraperitoneally (i.p.). For challenge with vaccinia virus, 2 × 10^6 PFU of VV-WR was diluted in PBS and injected i.v. Secondary memory cells were generated by immunization with OVA protein-coated splenocytes followed by boosting with LM-OVA 1 week later (Pham et al., 2010).

Flow Cytometry and Cell Sorting

For surface phenotype experiments, cells were stained with the following antibodies from eBioscience or BD Biosciences unless otherwise noted: CD8$^+$ (53-6.7), CD44 (IM7), CD43 (glycoform sensitive antibody, 1B11; Biolegend), CD27 (LG.7F9), KLRG1 (2F1), CD62L (MEL-14), CD122 (TMb1), CD127 (A7R34), and CXCR3 (CXCR3-173; Biolegend). The gp33-D^b, OVA-K^b, and B8R-K^b tetramers were generated as previously described (Daniels and Jameson, 2000) or were provided by the NIH Tetramer Facility. For intracellular staining, cells were fixed and permeabilized with Foxp3 Fixation and Permeabilization Buffers (eBioscience) and stained with antibodies to T-bet (4B10), Eomesodermin (Dan11mag), and Granzyme B (MHGB04; Invitrogen) for 1 hr at 4°C in Permeabilization Solution. Flow cytometry data were analyzed by using FlowJo analysis software. Intraepithelial and Lamina Propria cells of the small intestine were isolated as previously described (Casey et al., 2012; Masopust et al., 2010).

For cell sorting, spleen or spleen and lymph nodes were harvested from mice >30 days after infection with LCMV or LM. Collagenase digestion was performed on tissues followed by negative enrichment for CD8$^+$ T cells by using Miltenyi enrichment antibody cocktail and beads. Cells were then stained with CD8$^+$, CD44, CD27, and CD43 and sorted into populations by using a FACSAria. Purity was confirmed and, where applicable, the number of antigen-specific cells within each subset was determined by using tetramer staining or analysis with relevant congenic markers. Next, 2–3 × 10^4 cells of the indicated phenotype were injected (i.v.) into naive, congenically distinct hosts, which were infected (as indicated) 1 day later.

Flow Cytometric Discrimination of Cells in Splenic White and Red Pulp

As described (Anderson et al., 2012; Galkina et al., 2005; Teijaro et al., 2011), mice were first injected i.v. with fluorescently labeled anti-CD8$^+\alpha$ antibody. The animals were sacrificed 3 min later, a splenocytes single-cell suspension was prepared, and the cells were stained again for CD8$^+\alpha$, by using a distinct fluorochrome conjugate, and simultaneously stained for other cell surface markers. In some experiments, mice were perfused immediately after sacrifice, with similar findings. As shown by others (Anderson et al., 2012), cells in contact with the blood circulation (including the splenic red pulp) are labeled by the intravenously injected anti-CD8$^+$ antibody, while cells in parenchymal locations (including the splenic white pulp) are not.

In Vitro Stimulations

Sorted memory CD8$^+$ T cells (P14 or OT-1) were incubated with peptide (KAVYNFATM or SIINFEKL), and Brefeldin A (BD Biosciences) for 5 to 6 hr. Following surface staining, cells were fixed and permeabilized with BD Cytofix and Cytoperm (Becton Dickinson) followed by intracellular staining for IFN-γ, TNF, and IL-2 in BD Perm Wash Buffer (Becton Dickinson) (Hamilton et al., 2006). Cytokine stimulations with IL-2, IL-12, and IL-18 were performed as described previously (Haluszczak et al., 2009).

Determination of Colony-Forming Units and Cell Expansion

This was performed as previously described (Hamilton et al., 2006, 2010). Briefly, on day 5 after infection, the spleen and liver were removed and placed in a 0.2% IGEPAL solution (Sigma-Aldrich). Organs were homogenized, and serial dilutions were plated onto TSB plates containing 50 μg/ml streptomycin.

Bacterial colonies were counted following plate incubation for ~24 hr at 37°C. The limit of detection (approximately 100 organisms) is indicated on graphs by a dashed line. To determine the number of transferred cells in recipient mice, splenic single-cell suspensions were counted and stained with antibodies to CD8+, CD44, and CD45.2 (104) or Thy1.1 (HIS51) (to identify donor cells) and, in some cases, relevant peptide-MHC tetramer. In some experiments, no-transfer control groups were used to determine the limit of donor cell detection.

Plaque Assay

This was performed as previously described (Hamilton et al., 2010). Briefly, on day 3 after infection with VV-WR, ovaries were harvested in PBS and frozen as a single-cell suspension. After two freeze-thaw cycles, the ovary homogenate was incubated at 37°C for 45 min with 0.25 mg/ml trypsin (Sigma). 143B cells (ATCC) were grown to confluence. Dilutions of the ovary homogenate were added in duplicate to the cellular monolayer and left for two days. Staining with 1% crystal violet was then performed. Plaques were counted and total viral load per ovaries was calculated.

Statistics

A two-tailed, unpaired, Student's t test was performed on log transformed data, by using Prism (GraphPad Software). In some figures, p values are represented as follows: ***$p < 0.001$; **$p < 0.01$; *$p < 0.05$.

SUPPLEMENTAL INFORMATION

Supplemental Information includes five figures and can be found with this article online at http://dx.doi.org/10.1016/j.immuni.2013.05.009.

ACKNOWLEDGMENTS

We thank the Masopust laboratory (especially Kristin Anderson) for help establishing splenic localization assays and timely provision of aged memory P14 CD8+ T cells, Josiah Zacharias for valuable experimental input, and the University of Minnesota Flow Core personnel for cell sorting. We are grateful to Kris Hogquist, Matt Mescher, Dave Masopust, Dietmar Zehn, Stephen McSorley, and members of the Jamequist laboratory for mouse and bacterial strains and helpful discussions. This work was supported by the National Institutes of Health (grants R01AI75168 and R37AI38903 to S.C.J., and Cancer Biology Postdoctoral Training Grant 5T32CA009138-38 to J.A.O) and a Leukemia and Lymphoma Career Development Award (to S.E.H.).

Received: August 1, 2012
Accepted: May 16, 2013
Published: June 6, 2013

REFERENCES

Anderson, K.G., Sung, H., Skon, C.N., Lefrancois, L., Deisinger, A., Vezys, V., and Masopust, D. (2012). Cutting edge: intravascular staining redefines lung CD8 T cell responses. J. Immunol. *189*, 2702–2706.

Aoshi, T., Carrero, J.A., Konjufca, V., Koide, Y., Unanue, E.R., and Miller, M.J. (2009). The cellular niche of Listeria monocytogenes infection changes rapidly in the spleen. Eur. J. Immunol. *39*, 417–425.

Baars, P.A., Sierro, S., Arens, R., Tesselaar, K., Hooibrink, B., Klenerman, P., and van Lier, R.A. (2005). Properties of murine (CD8+)CD27- T cells. Eur. J. Immunol. *35*, 3131–3141.

Bachmann, M.F., Wolint, P., Schwarz, K., Jäger, P., and Oxenius, A. (2005a). Functional properties and lineage relationship of CD8+ T cell subsets identified by expression of IL-7 receptor alpha and CD62L. J. Immunol. *175*, 4686–4696.

Bachmann, M.F., Wolint, P., Schwarz, K., and Oxenius, A. (2005b). Recall proliferation potential of memory CD8+ T cells and antiviral protection. J. Immunol. *175*, 4677–4685.

Badovinac, V.P., Messingham, K.A., Jabbari, A., Haring, J.S., and Harty, J.T. (2005). Accelerated CD8+ T-cell memory and prime-boost response after dendritic-cell vaccination. Nat. Med. *11*, 748–756.

Bajénoff, M., Narni-Mancinelli, E., Brau, F., and Lauvau, G. (2010). Visualizing early splenic memory CD8+ T cells reactivation against intracellular bacteria in the mouse. PLoS ONE *5*, e11524.

Banerjee, A., Gordon, S.M., Intlekofer, A.M., Paley, M.A., Mooney, E.C., Lindsten, T., Wherry, E.J., and Reiner, S.L. (2010). Cutting edge: The transcription factor eomesodermin enables CD8+ T cells to compete for the memory cell niche. J. Immunol. *185*, 4988–4992.

Berg, R.E., Crossley, E., Murray, S., and Forman, J. (2003). Memory CD8+ T cells provide innate immune protection against Listeria monocytogenes in the absence of cognate antigen. J. Exp. Med. *198*, 1583–1593.

Casey, K.A., Fraser, K.A., Schenkel, J.M., Moran, A., Abt, M.C., Beura, L.K., Lucas, P.J., Artis, D., Wherry, E.J., Hogquist, K., et al. (2012). Antigen-independent differentiation and maintenance of effector-like resident memory T cells in tissues. J. Immunol. *188*, 4866–4875.

Daniels, M.A., and Jameson, S.C. (2000). Critical role for CD8 in T cell receptor binding and activation by peptide/major histocompatibility complex multimers. J. Exp. Med. *191*, 335–346.

Edwards, L.E., Haluszczak, C., and Kedl, R.M. (2013). Phenotype and function of protective, CD4-independent CD8 T cell memory. Immunol. Res. *55*, 135–145.

Galkina, E., Thatte, J., Dabak, V., Williams, M.B., Ley, K., and Braciale, T.J. (2005). Preferential migration of effector CD8+ T cells into the interstitium of the normal lung. J. Clin. Invest. *115*, 3473–3483.

Haluszczak, C., Akue, A.D., Hamilton, S.E., Johnson, L.D., Pujanauski, L., Teodorovic, L., Jameson, S.C., and Kedl, R.M. (2009). The antigen-specific CD8+ T cell repertoire in unimmunized mice includes memory phenotype cells bearing markers of homeostatic expansion. J. Exp. Med. *206*, 435–448.

Hamilton, S.E., Wolkers, M.C., Schoenberger, S.P., and Jameson, S.C. (2006). The generation of protective memory-like CD8+ T cells during homeostatic proliferation requires CD4+ T cells. Nat. Immunol. *7*, 475–481.

Hamilton, S.E., Schenkel, J.M., Akue, A.D., and Jameson, S.C. (2010). IL-2 complex treatment can protect naive mice from bacterial and viral infection. J. Immunol. *185*, 6584–6590.

Hansen, S.G., Vieville, C., Whizin, N., Coyne-Johnson, L., Siess, D.C., Drummond, D.D., Legasse, A.W., Axthelm, M.K., Oswald, K., Trubey, C.M., et al. (2009). Effector memory T cell responses are associated with protection of rhesus monkeys from mucosal simian immunodeficiency virus challenge. Nat. Med. *15*, 293–299.

Hansen, S.G., Ford, J.C., Lewis, M.S., Ventura, A.B., Hughes, C.M., Coyne-Johnson, L., Whizin, N., Oswald, K., Shoemaker, R., Swanson, T., et al. (2011). Profound early control of highly pathogenic SIV by an effector memory T-cell vaccine. Nature *473*, 523–527.

Heffner, M., and Fearon, D.T. (2007). Loss of T cell receptor-induced Bmi-1 in the KLRG1(+) senescent CD8(+) T lymphocyte. Proc. Natl. Acad. Sci. USA *104*, 13414–13419.

Hikono, H., Kohlmeier, J.E., Ely, K.H., Scott, I., Roberts, A.D., Blackman, M.A., and Woodland, D.L. (2006). T-cell memory and recall responses to respiratory virus infections. Immunol. Rev. *211*, 119–132.

Hikono, H., Kohlmeier, J.E., Takamura, S., Wittmer, S.T., Roberts, A.D., and Woodland, D.L. (2007). Activation phenotype, rather than central- or effector-memory phenotype, predicts the recall efficacy of memory CD8+ T cells. J. Exp. Med. *204*, 1625–1636.

Hogquist, K.A., Jameson, S.C., Heath, W.R., Howard, J.L., Bevan, M.J., and Carbone, F.R. (1994). T cell receptor antagonist peptides induce positive selection. Cell *76*, 17–27.

Huster, K.M., Stemberger, C., Gasteiger, G., Kastenmüller, W., Drexler, I., and Busch, D.H. (2009). Cutting edge: memory CD8 T cell compartment grows in size with immunological experience but nevertheless can lose function. J. Immunol. *183*, 6898–6902.

Intlekofer, A.M., Takemoto, N., Wherry, E.J., Longworth, S.A., Northrup, J.T., Palanivel, V.R., Mullen, A.C., Gasink, C.R., Kaech, S.M., Miller, J.D., et al. (2005). Effector and memory CD8+ T cell fate coupled by T-bet and eomesodermin. Nat. Immunol. *6*, 1236–1244.

Intlekofer, A.M., Takemoto, N., Kao, C., Banerjee, A., Schambach, F., Northrop, J.K., Shen, H., Wherry, E.J., and Reiner, S.L. (2007). Requirement for T-bet in the aberrant differentiation of unhelped memory CD8+ T cells. J. Exp. Med. *204*, 2015–2021.

Jabbari, A., and Harty, J.T. (2006). Secondary memory CD8+ T cells are more protective but slower to acquire a central-memory phenotype. J. Exp. Med. *203*, 919–932.

Jameson, S.C., and Masopust, D. (2009). Diversity in T cell memory: an embarrassment of riches. Immunity *31*, 859–871.

Joshi, N.S., Cui, W., Chandele, A., Lee, H.K., Urso, D.R., Hagman, J., Gapin, L., and Kaech, S.M. (2007). Inflammation directs memory precursor and short-lived effector CD8(+) T cell fates via the graded expression of T-bet transcription factor. Immunity *27*, 281–295.

Jung, Y.W., Rutishauser, R.L., Joshi, N.S., Haberman, A.M., and Kaech, S.M. (2010). Differential localization of effector and memory CD8 T cell subsets in lymphoid organs during acute viral infection. J. Immunol. *185*, 5315–5325.

Kaech, S.M., and Wherry, E.J. (2007). Heterogeneity and cell-fate decisions in effector and memory CD8+ T cell differentiation during viral infection. Immunity *27*, 393–405.

Kaech, S.M., Tan, J.T., Wherry, E.J., Konieczny, B.T., Surh, C.D., and Ahmed, R. (2003). Selective expression of the interleukin 7 receptor identifies effector CD8 T cells that give rise to long-lived memory cells. Nat. Immunol. *4*, 1191–1198.

Kambayashi, T., Assarsson, E., Lukacher, A.E., Ljunggren, H.G., and Jensen, P.E. (2003). Memory CD8+ T cells provide an early source of IFN-gamma. J. Immunol. *170*, 2399–2408.

Karupiah, G., Coupar, B., Ramshaw, I., Boyle, D., Blanden, R., and Andrew, M. (1990). Vaccinia virus-mediated damage of murine ovaries and protection by virus-expressed interleukin-2. Immunol. Cell Biol. *68*, 325–333.

Laouar, A., Manocha, M., Haridas, V., and Manjunath, N. (2008). Concurrent generation of effector and central memory CD8 T cells during vaccinia virus infection. PLoS ONE *3*, e4089.

Masopust, D., Ha, S.J., Vezys, V., and Ahmed, R. (2006a). Stimulation history dictates memory CD8 T cell phenotype: implications for prime-boost vaccination. J. Immunol. *177*, 831–839.

Masopust, D., Vezys, V., Wherry, E.J., Barber, D.L., and Ahmed, R. (2006b). Cutting edge: gut microenvironment promotes differentiation of a unique memory CD8 T cell population. J. Immunol. *176*, 2079–2083.

Masopust, D., Vezys, V., Wherry, E.J., and Ahmed, R. (2007). A brief history of CD8 T cells. Eur. J. Immunol. *37*(*Suppl 1*), S103–S110.

Masopust, D., Choo, D., Vezys, V., Wherry, E.J., Duraiswamy, J., Akondy, R., Wang, J., Casey, K.A., Barber, D.L., Kawamura, K.S., et al. (2010). Dynamic T cell migration program provides resident memory within intestinal epithelium. J. Exp. Med. *207*, 553–564.

Messingham, K.A., Badovinac, V.P., and Harty, J.T. (2003). Deficient antilisterial immunity in the absence of perforin can be restored by increasing memory CD8+ T cell numbers. J. Immunol. *171*, 4254–4262.

Nolz, J.C., and Harty, J.T. (2011). Protective capacity of memory CD8+ T cells is dictated by antigen exposure history and nature of the infection. Immunity *34*, 781–793.

Nolz, J.C., Rai, D., Badovinac, V.P., and Harty, J.T. (2012). Division-linked generation of death-intermediates regulates the numerical stability of memory CD8 T cells. Proc. Natl. Acad. Sci. USA *109*, 6199–6204.

Obar, J.J., and Lefrançois, L. (2010). Early signals during CD8 T cell priming regulate the generation of central memory cells. J. Immunol. *185*, 263–272.

Pham, N.L., Pewe, L.L., Fleenor, C.J., Langlois, R.A., Legge, K.L., Badovinac, V.P., and Harty, J.T. (2010). Exploiting cross-priming to generate protective CD8 T-cell immunity rapidly. Proc. Natl. Acad. Sci. USA *107*, 12198–12203.

Pircher, H., Rohrer, U.H., Moskophidis, D., Zinkernagel, R.M., and Hengartner, H. (1991). Lower receptor avidity required for thymic clonal deletion than for effector T-cell function. Nature *351*, 482–485.

Pope, C., Kim, S.K., Marzo, A., Masopust, D., Williams, K., Jiang, J., Shen, H., and Lefrançois, L. (2001). Organ-specific regulation of the CD8 T cell response to Listeria monocytogenes infection. J. Immunol. *166*, 3402–3409.

Prlic, M., and Bevan, M.J. (2008). Exploring regulatory mechanisms of CD8+ T cell contraction. Proc. Natl. Acad. Sci. USA *105*, 16689–16694.

Prlic, M., Sacks, J.A., and Bevan, M.J. (2012). Dissociating markers of senescence and protective ability in memory T cells. PLoS ONE *7*, e32576.

Rutishauser, R.L., and Kaech, S.M. (2010). Generating diversity: transcriptional regulation of effector and memory CD8 T-cell differentiation. Immunol. Rev. *235*, 219–233.

Sallusto, F., Lenig, D., Förster, R., Lipp, M., and Lanzavecchia, A. (1999). Two subsets of memory T lymphocytes with distinct homing potentials and effector functions. Nature *401*, 708–712.

Sallusto, F., Geginat, J., and Lanzavecchia, A. (2004). Central memory and effector memory T cell subsets: function, generation, and maintenance. Annu. Rev. Immunol. *22*, 745–763.

Sandau, M.M., Kohlmeier, J.E., Woodland, D.L., and Jameson, S.C. (2010). IL-15 regulates both quantitative and qualitative features of the memory CD8 T cell pool. J. Immunol. *184*, 35–44.

Sarkar, S., Kalia, V., Haining, W.N., Konieczny, B.T., Subramaniam, S., and Ahmed, R. (2008). Functional and genomic profiling of effector CD8 T cell subsets with distinct memory fates. J. Exp. Med. *205*, 625–640.

Seder, R.A., Darrah, P.A., and Roederer, M. (2008). T-cell quality in memory and protection: implications for vaccine design. Nat. Rev. Immunol. *8*, 247–258.

Slifka, M.K., and Whitton, J.L. (2001). Functional avidity maturation of CD8(+) T cells without selection of higher affinity TCR. Nat. Immunol. *2*, 711–717.

Teijaro, J.R., Turner, D., Pham, Q., Wherry, E.J., Lefrançois, L., and Farber, D.L. (2011). Cutting edge: Tissue-retentive lung memory CD4 T cells mediate optimal protection to respiratory virus infection. J. Immunol. *187*, 5510–5514.

Vezys, V., Yates, A., Casey, K.A., Lanier, G., Ahmed, R., Antia, R., and Masopust, D. (2009). Memory CD8 T-cell compartment grows in size with immunological experience. Nature *457*, 196–199.

Wherry, E.J., Teichgräber, V., Becker, T.C., Masopust, D., Kaech, S.M., Antia, R., von Andrian, U.H., and Ahmed, R. (2003). Lineage relationship and protective immunity of memory CD8 T cell subsets. Nat. Immunol. *4*, 225–234.

Williams, M.A., and Bevan, M.J. (2007). Effector and memory CTL differentiation. Annu. Rev. Immunol. *25*, 171–192.

Wirth, T.C., Harty, J.T., and Badovinac, V.P. (2010a). Modulating numbers and phenotype of CD8+ T cells in secondary immune responses. Eur. J. Immunol. *40*, 1916–1926.

Wirth, T.C., Xue, H.H., Rai, D., Sabel, J.T., Bair, T., Harty, J.T., and Badovinac, V.P. (2010b). Repetitive antigen stimulation induces stepwise transcriptome diversification but preserves a core signature of memory CD8(+) T cell differentiation. Immunity *33*, 128–140.

Wolint, P., Betts, M.R., Koup, R.A., and Oxenius, A. (2004). Immediate cytotoxicity but not degranulation distinguishes effector and memory subsets of CD8+ T cells. J. Exp. Med. *199*, 925–936.